Evaluation of a simple approach for crop evapotranspiration partitioning and analysis of the water budget distribution for several crop species

Pierre Beziat, Vincent Rivalland, Tiphaine Tallec, Nathalie Jarosz, Gilles Boulet, P. Gentine, Eric Ceschia

Evaluation of a simple approach for crop evapotranspiration partitioning and analysis of the water budget distribution for several crop species

Pierre Béziat [a], Vincent Rivalland [a,*], Tiphaine Tallec [a], Nathalie Jarosz [a], Gilles Boulet [a], Pierre Gentine [b], Eric Ceschia [a]

[a] *Centre d'Etudes Spatiales de la BIOsphère (CESBIO), 18 avenue Edouard Belin bpi 2801, 31401 Toulouse cedex 9, France*

[b] *Department of Earth and Environmental Engineering, Columbia University, New York, NY 10027, USA*

* Corresponding author:

Mail: Centre d'Etudes Spatiale de la BIOsphère (CESBIO),

18 Avenue Edouard Belin bpi 2801,

31401 Toulouse cedex 9, France

Email: vincent.rivalland@cesbio.cnes.fr

Abstract

Climate variability and climate change induce important intra- and inter-annual variability of precipitation that significantly alters the hydrologic cycle. The surface water budgets and the plant or ecosystem water use efficiency (WUE) are in turn modified. Obtaining greater insight into how climatic variability and agricultural practices affect water budgets and regarding their components in croplands is, thus, important for adapting crop management and limiting water losses. Therefore, the principal objectives of this study are:

1) to assess the contribution of different components to the agro-ecosystem water budget and
2) to evaluate how agricultural practices and climate modify the components of the surface water budget.

To achieve these goals, we tested a new method for partitioning evapotranspiration (ETR), measured by means of an eddy-covariance method, into soil evaporation (E) and plant transpiration (TR) based on marginal distribution sampling (MDS). The partitioning method proposed requires continuous flux recording and measurements of soil temperature and humidity close to the surface, global radiation above the canopy and assessment of leaf area index dynamics. This method is well suited for crops because it requires a dataset including long bare-soil periods alternating with vegetated periods for accurate partitioning estimation.

We compared these estimations with calibrated simulations of the ICARE-SVAT double source mechanistic model.The results showed good agreement between the two partitioning methods, demonstrating that MDS is a convenient, simple and robust tool for estimating E with reasonable associated uncertainties. During the growing season, the proportion of E in ETR was approximately one-third and varied mainly with crop leaf area. When calculated on an annual time scale, the proportion of E in ETR reached more than 50%, depending on the crop leaf area and on the duration and distribution of bare soil within the year.

Keywords

Crop; Evapotranspiration; Transpiration; Evaporation; Water budget; Partitioning; land-surface model

1. Introduction

Agricultural water resource limitations have become a major issue as the Earth's population has drastically increased, leading to a corresponding increase in food demand. Furthermore, global climate change will locally impact the mean and variance of temperature as well as the amount and distribution of precipitation and atmospheric CO_2 concentrations (IPCC, 2007). Agriculture will be strongly impacted by these changes (Brouder and Volenec, 2008). In this context, quantifying and understanding the drivers of the water cycle components, such as climate variability, climate change and crop rotations, are essential for facing both agro-economic and environmental challenges.

Allen (2008) documented methods related to the calculation of evapotranspiration (ETR), from experimental and modeling methods using different time and space scales. For all of these methods, which spatial scales ranged from local soil water sampling, lysimeters and eddy covariance (EC) to scintillometry, the reality that an improperly designed experiment or measurement can lead to highly erroneous water use estimates is evident. For ETR partitioning between evaporation (E) and transpiration (TR), sapflow measurements (Granier et al., 1996; Roupsard et al., 2006; Steppe et al., 2010) and isotope techniques (Williams et al., 2004) combined with EC measurements over forests have been used to estimate E and TR at the canopy scale. In other studies, two levels of EC measurements have been used to infer the TR and WUE of the forest canopy itself (Jarosz et al., 2008; Lamaud et al., 1996; Roupsard et al., 2006), as fluxes from the soil and understory can constitute a significant portion of the total ecosystem flux. Over croplands, gas exchange measurements at the leaf scale (Medrano et al., 2009; Steduto and Albrizio, 2005; Steduto et al., 1997) and lysimeter measurements (Qiu et al., 2008; Steiner and Hatfield, 2008) have also been used to analyse the different components of ETR at the plant or canopy scale.

Empirical modeling approaches based on energy balance formulations have been used to estimate TR (Li et al., 2008; Ritchie, 1972), but large differences compared to TR estimation using sapflow measurements have been observed (Sauer et al., 2007). When using mechanistic modeling to infer TR, one-source (vegetation plus soil as a whole) (Chen et al., 1996; Koren et al., 1999; Noilhan and Mahfouf, 1996; Noilhan and Planton, 1989), two-source (soil plus vegetation, separately) (Gentine et al., 2007; Hu et al., 2009; Sellers et al., 1996; Shuttleworth and Wallace, 1985), three-source (bare soil, shaded soil and vegetation) (Boulet et al., 1999), or multiple-source (Ogée et al., 2003) soil vegetation atmosphere transfer (SVAT) models can be used. The use of two (or more) sources in models allows for a more realistic representation of the energy budget and can describe the respective contributions of the soil and vegetation to ETR. However, although more complex SVATs may be more mechanistic, they require more input parameters, which involve complicated calibrations and often the solution might be ill-defined (Beven, 2006). If the complex model is calibrated over a short

period and with too few observed variables, a correct ETR can be obtained with incorrect E-TR partitioning. The right answer is obtained yet for the wrong reason. All of these TR estimation methods raise questions regarding their spatial representativeness, the generalization of their applicability, and the complexity of the modeling tools used.

In the present study, the main objectives are 1) to assess the different components of the annual crop water budget and 2) to evaluate a simple and generic method for partitioning ETR into soil and vegetation components. The advantage of such simple method is that it can be easily used in other regions with minimum calibration effort. The obtained result is thus more robust than more complex models, which would require recalibration.

EC measurements of water fluxes were performed continuously over a period of 2 years above winter and summer crops in the southwest of France to highlight the contribution of each component to the agro-ecosystem water budget and the impact of different crop species in relation to climatic conditions on each of them. From these measurements, we developed a new methodology based on marginal distribution sampling (MDS) to infer the partitioning of ETR between E and TR during each crop growing season. We evaluated this methodology against actual data during bare soil periods for E and against a site-calibrated mechanistic modeling approach using the ICARE-SVAT model (Gentine et al., 2007) for both bare soil and vegetated periods.

2. Materials and methods

2.1. Site and measurement descriptions

Since March 2005, micrometeorological, meteorological and vegetation dynamic measurements have been performed at two cultivated plots located 12 km apart near Toulouse in the southwestern part of France located at Auradé (43°54'97''N, 01°10'61''E) and Lamasquère (43°49'65''N, 01°23'79''E). Both sites are part of the CarboEurope-IP Regional Experiment (Dolman et al., 2006) and the CarboEurope-IP Ecosystem Component. They have been cultivated for more than 30 years, and they experience similar meteorological conditions but are subjected to different management practices and exhibit different soil properties and topography. The crop rotations on both sites are representative of the main regional crop rotations. Crops from the 2005-06 and 2006-07 growing seasons were analyzed in this study. Each crop year was studied on the basis of the hydrologic year, *i.e.*, from the 1st of October, after the summer crop harvest and before the beginning of winter crop sowing at the end of November. The Auradé plot was cultivated with winter wheat (*Triticum aestivum L.*) from 27 October 2005 to 29 June 2006 followed by sunflower (*Helianthus annuus L.*) from 11 April 2007 to 20 September 2007. The Lamasquère plot was cultivated with maize (*Zea mays L.*) used for silaging from the 1st of May 2006 to 31 August 2006 followed by winter wheat from 18 October 2006 to 15 July 2007. The Lamasquère site was irrigated in 2006 when maize was cultivated.

Turbulent fluxes of water vapor (ETR and latent heat, LE), sensible heat (H) and momentum (τ) were measured continuously by the EC method (Aubinet et al., 2000; Baldocchi, 2003; Grelle and Lindroth, 1996; Moncrieff et al., 1997). EC devices were mounted at heights of 2.8 m at Auradé and 3.65 m at Lamasquère. The instrument heights were chosen to be at least 1 m higher than the crops at the time of their maximum development. The EC system consists of a three-dimensional sonic anemometer (CSAT 3, Campbell Scientific Inc., Logan, UT, USA) and an open-path infrared gas analyzer (LI7500, LiCor, Lincoln, NE, USA). EdiRe software (Robert Clement, © 1999, University of Edinburgh, UK) was used to calculate fluxes following CarboEurope-IP recommendations. A 2D rotation was applied to align the stream-wise wind velocity component with the direction of the mean velocity vector. Fluxes were corrected for spectral frequency loss (Moore, 1986). Water fluxes were corrected for air density variations (Webb et al., 1980). Flux filtering, quality controls and gap filling were performed following CarboEurope-IP recommendations.

Standard meteorological variables in the air and in the soil were recorded at each site to analyze and correct turbulent fluxes. Destructive vegetation measurements were performed regularly

to follow biomass and surface vegetation area dynamics. A complete description of the site characteristics, management practices, biomass inventories, vegetation area measurements, instrumentation setups, flux filtering, quality controls and gap filling procedures is available in Béziat et al. (2009).

2.2. Evapotranspiration partitioning between soil evaporation and vegetation transpiration

A statistical methodology based on marginal distribution sampling (MDS) (Reichstein et al., 2005) has been designed to partition ETR between E and TR using meteorological variables. The general principle of MDS consists of estimating flux data using the mean of the fluxes under similar meteorological conditions by construction of a look-up table.

To access the partition of ETR during the vegetation period, we first construct an MDS dataset linking measured ETR values with meteorological variables during bare soil periods (when ETR is reduced to its E component). Note that, for building the look-up table, we did not use a time moving window as in Reichstein et al. (2005) but the maximum of available data during the bare soil periods before or after the vegetated period. As a result, we estimated E during the period with vegetation using MDS (E_{MDS}) with a similar range of driving variables. Bare soil periods were defined as the period between tillage and sowing. Periods immediately following harvesting, when stubble was still on the ground or when regrowth events occurred, were discarded from the MDS calculation dataset. Table 1 describes the bare soil periods and the corresponding filtered ETR data available for the calculation of E_{MDS}. Vegetation periods were defined for a leaf area index (LAI) threshold above 0.2 m^2 m^{-2} during daytime. Outside of these periods, TR was assumed to be negligible, and E was considered to be equal to the gap-filled ETR measurements.

Three variables that can be measured or estimated during both bare soil and vegetation periods were considered as driving factors for E: soil water content at a 5 cm depth (SWC_5), temperature at a 5 cm depth (T_{s5}) and net short wave radiation reaching the ground surface (RG_s). We choose not to consider relative humidity and wind speed as driving factors because the first was too difficult to model close to the ground in a fast growing stand and the second is supposed to vanish close to the ground surface during the whole vegetated periods. Additionally, our objective was to test a method that could be easily applied at sites that are equipped with instruments for standard micrometeorological measurements.

The bare soil periods occurred during winter and spring before the summer crop season and during summer and autumn before the winter crop season (Table 1). Therefore, even if bare soil periods are shifted in time compared to growing periods, the ranges of SWC_5, T_{s5} and RG_s encountered during these periods were assumed to be sufficiently large for the calculation of E by

MDS during vegetated periods. To set up E_{MDS}, the E-driving variables space was split into regular intervals; the initial ranges of these intervals were at first fixed at 2 % for SWC_5, 1 °C for T_{s5} and 25 W m^{-2} for RG_s. As these ranges did not permit the construction of a complete E_{MDS} dataset, they were increased progressively to threshold values of 8 %, 4 °C and 100 W m^{-2} by steps of 2 %, 1 °C and 25 W m^{-2} for SWC_5, T_{s5} and RG_s, respectively. If E_{MDS} was still incomplete (14.5 % and 10.5 % of the E_{MDS} data were missing after this step at Auradé and Lamasquère, respectively), the standard gap-filling algorithm defined by Reichstein et al. (2005) and adapted by Béziat et al. (2009) to account for discontinuity in the field status corresponding to crop functioning periods between dates of sowing, maximum crop development, harvest and tillage was applied using SWC_5, T_{s5} and RG_s as driving variables. Then, during vegetation periods, TR was estimated (TR_{MDS}) as the difference between gap-filled ETR and E_{MDS}.

As RG_s was not measured directly at ground height during vegetation periods, the two-layer (soil and vegetation) radiative transfer formulation described by Taconet et al. (1986) was used for its estimation:

Erreur ! Erreur !(4)

where RG is the incident short wave solar radiation at the top of the canopy, a_s is the soil albedo, a_v is the vegetation albedo, and σ_f is a shielding factor representing the ratio of radiation intercepted by the vegetation. A mean value of 0.15 for a_s was calculated from incident and reflected RG measurements during the bare soil periods defined above using a CNR1 (Kipp & Zonen, Delft, NL). Temporal dynamics of a_v were calculated based on the proportions of green leaf area index (LAI_g) and senescent (yellow) LAI (LAI_y) compared to total LAI ($LAI_{tot} = LAI_g + LAI_y$):

Erreur !Erreur !(5)

where a_g and a_y indicate the albedo of green and senescent vegetation, respectively. For all crops, a mean value of 0.2 for a_g and 0.25 for a_y was estimated following Hartmann (1994). Continuous LAI_g values were obtained by spline interpolation of destructive LAI measurements performed monthly during the slow growing period and every two weeks during the fast growing period (Béziat et al., 2009). LAI_y dynamic was estimated based on the maximum LAI_g (LAI_{max}) as follows:

$$LAI_y = r \cdot LAI_{max} - LAI_g \quad (6)$$

where r is the LAI reduction coefficient accounting for surface losses caused by the falling and drying of leaves during senescence. We considered r as varying linearly from 1 at LAI_{max} to 0.8 at harvesting. Calculation of σ_f was carried out by means of a Beer-Lambert-type law:

192 $$\sigma_f = 1 - e^{(-k \cdot LAI_{tot})} \quad (7)$$

193 where k is the extinction coefficient according to the incident direction ($\Omega_s = (\theta_s,\varphi_s)$, described by the
194 zenithal and azimuthal solar angles, respectively). The k formulation proposed by Goudriaan (1977)
195 was used:

196 **Erreur !Erreur !**(8)

197 where $G(\Omega_s)$ indicates the ratio of effective LAI_{tot}, according to Ω_s. In our case, leaf orientation was
198 assumed to be azimuthally symmetrical and spherical, and therefore, $G(\Omega_s) = G(\theta_s) = 0.5$. The $\sqrt{1-a_v}$
199 term was introduced by Goudriaan (1977) to account for the influence of diffusion on transmittance.

200 ## 2.3. SVAT model description and calibration

201 The model proposed in this study as a second approach to evaluate the partitioning of ETR
202 into TR and E is the Soil Vegetation Atmosphere Transfer (SVAT) model known as ICARE (Gentine
203 et al., 2007). This model was developed to provide as physical as possible a representation of the main
204 processes involved in the soil-plant-atmosphere system. Two layers are considered at the surface: one
205 for vegetation and one for the underlying bare soil. The energy budget is solved for each component
206 according to Shuttleworth and Wallace (1985) and as described in Braud et al. (1995). The soil is
207 divided into two reservoirs, a surface reservoir and a deep reservoir with a water balance formalism
208 based on the original ISBA scheme (Noilhan and Mahfouf, 1996; Noilhan and Planton, 1989). The soil
209 water content and temperature dynamics are solved following the *force-restore* method applied by
210 Deardorff (1977). ETR and H flux are controlled by a succession of resistances that provide a simple,
211 yet physically realistic description of the transition of energy and mass between bare soil and the
212 closed canopy. There are five resistances involved in this model (Figure 1): the canopy stomatal
213 resistance (r_{sto}, s m^{-1}), the soil surface resistance (r_{ss}, s m^{-1}), the aerodynamic resistance between the
214 ground surface and the top of the canopy (r_{as}, s m^{-1}), the canopy boundary layer resistance (r_{ac}, s m^{-1})
215 and the aerodynamic resistance between the top of the canopy and a reference level above the canopy
216 (r_a, s m^{-1}). All aerodynamic resistances are based on Choudhury and Monteith (1988) and include the
217 atmospheric static-stability correction based on Monin-Obukhov Similarity Theory (MOST).
218 Three resistances are critical for this study because of their contribution to partitioning ETR
219 between E and TR. The first resistance is r_{ss}, which controls soil E. It was formulated as an
220 exponential function of the relative surface soil water content (Passerat De Silans et al., 1989):

221 **Erreur !Erreur !**(9)

where SWC_s and SWC_{sat} represent the near-surface soil water content and soil porosity (m^3 m^{-3}), respectively, and A_{rss} is an empirical factor. r_{ss} exponentially increase with soil drying. The second resistance is r_{sto}, which is extremely important for the canopy state variable dynamics law that primarily controls TR. The r_{sto} parameter was expressed following the classic Jarvis (1976) representation as presented in Noilhan and Planton (1989):

Erreur !Erreur !(10)

where r_{smin} is the minimum stomatal resistance function, and f_i are stress factors with values between 1 and 0, depending on global solar radiation (RG), water stress estimated from the current SWC in the rooting zone (SWC_r) and the SWC at the wilting point (SWC_{wilt}), the air vapor pressure deficit (VPD) and the temperature of the air and canopy (Ta and Tc, respectively). The use of bare soil and vegetated conditions allows nearly independent calibrations of the soil and canopy water resistances.

The third resistance is r_a, which controls both TR and E for water balance. It is calculated as in Brutsaert (1982):

Erreur !Erreur !(11)

where z_r and d are the reference and displacement heights, respectively; z_{0h} is the thermal roughness length; ψ_h represents the integral adiabatic correction function for heat; L_{mo} is the Monin-Obukhov length; K is the Von Karman constant; and u* is the friction velocity. In our application, z_{0h} is linked with z_0, the momentum ratio, by a constant ratio. For more details on resistance calculations and formalisms, see the appendix of Gentine et al. (2007).

To run the model and obtain reliable estimates of ETR partitioning, some variables measured *in situ* were forced as model inputs. These variables included 1) atmospheric variables (incoming shortwave radiation, precipitation, temperature and relative humidity of air and wind speed) measured routinely at each site at a half-hourly time intervals; 2) vegetation dynamic variables (LAI_g, LAI_y and vegetation height) at daily time intervals interpolated from *in situ* measurements (see section 2.2); and 3) the total (soil plus vegetation) mean daily albedo calculated as the ratio between outgoing and incoming shortwave radiation and measured at each site with a CNR1 (Kipp & Zonen, Delft, NL). Shortwave radiative transfer through the canopy was estimated following the same equations as employed for the calculation of RG_s in the MDS approach (Equations (4) to (8)). For longwave radiative transfer, the original ISBA formulation was used. Finally, the model calculates the dynamics of 1) the land-surface energy balance terms: net radiation (Rn), H, LE and its two components (E and TR) and soil heat flux (G); 2) the SWC of the two soil layers (the surface and rooting zones, with potential extraction fixed at 1.5 m for both sites); and 3) the surface and deep soil temperatures as well as canopy and radiative temperatures.

In this study, the model was adjusted to fit the main half-hourly components of the energy (Rn, LE and H) and water budgets (SWC) measured at both sites. We chose not to assimilate the measured SWC_5cm in the model to control soil surface conditions but to calibrate surface resistance to bare soil evaporation. As a result soil water budget is closed at both half-hourly and daily time step. Optimization of model outputs was performed independently for each site (Auradé and Lamasquère). Calibration of the model parameters was performed in two steps. The first step of optimization was based only on the bare soil periods defined in section 2.2 (Table 1) to fit r_{ss} and r_a. This soil calibration thus accounts for the site-specific soil response to E. Two parameters were considered as the most sensitive and significant: A_{rss} and the ratio z_0/z_{0h}, which are involved in the r_{ss} and r_a formulations (Equations (9) and (11)), respectively. The second step of optimization was performed for the vegetation periods to optimize the vegetation control on TR: r_{smin} and SWC_{wilt} (Equation (10)). Optimization was performed by maximizing the sum of the Nash criteria (Nash and Sutcliffe, 1970) for SWC, LE, H and Rn. The Nash criterion is given by:

Erreur !Erreur !(12)

where X represents the simulated data and Y the observed data. The Nash criterion has the advantage of being dimensionless, meaning that the addition of criteria gave the same importance to variables considered in the optimization process. The criterion is less sensitive than the root mean square error (RMSE) to extreme values. The values of the optimized parameters are summarized in Table 2. ETR, E and TR were finally modeled for each site using the mean of the best-fit parameters A_{rss} and the z_0/z_{0h} ratio for each bare soil period added to the best-fit parameters r_{smin} and SWC_{wilt} specific to each crop growing season.

2.4. Application and evaluation of the partitioning methods

Over bare soil periods (Table 1), it was possible to evaluate and compare soil E estimated by both the MDS approach and the ICARE-SVAT model simulations (E_{MDS} and E_{ICARE}, respectively). For this analysis, half-hourly data over bare soil were randomly split into two datasets: a calibration dataset and a validation dataset. For ICARE-SVAT, A_{rss} from r_{ss} and z_0/z_{0h} from r_a were fitted for each bare soil dataset at each site (Table 2) on the calibration dataset. Next, a simulation using the mean of the best fit parameters at each site was conducted to compare E estimations with the validation dataset. The same methodology was applied to the MDS method with the same randomly selected datasets. Note that, the dataset previously named calibration is there used for the construction of MDS. This exercise was carried out to compare the performance of the MDS method with that of ICARE-SVAT during bare soil periods. The results presented in Table 5 are discussed in section 3.3. We used the slope and the intercept of the linear regression, the determination coefficient (R^2), the root mean

square error (RMSE), the mean bias and the Nash criterion as statistical criteria to evaluate the partitioning methods and compare them with measurements. Thereafter, the complete bare soil dataset was used to calibrate MDS and ICARE-SVAT.

At the end of 2005 at Lamasquère, significant regrowth of weeds and previously harvested crops (Triticale) was observed on the plot between 1 October 2005 and 1December 2005, with the latter date corresponding to the date of ploughing. Consequently, a LAI_g of 0.7 m^2 m^{-2}, estimated from hemispherical photographs (Demarez et al., 2008) taken on 22 September 2005, was forced in both methods to estimate the partitioning between E and TR during this period. As the photographs were taken at the beginning of the regrowth event, the constant LAI value used over this two-month period was probably underestimated compared to the true LAI, even if growth was limited during this part of the year. However, this forcing was required for ICARE-SVAT to estimate a more reliable annual ETR.

In the ICARE-SVAT model, the evaporation of water intercepted by vegetation is taken into account by the filling of a foliar reservoir which maximum capacity by unit of soil depends on the type of crop, the LAI value and the leaf effective fraction for interception (Dickinson 1984). Following Deardorff (1978), the fraction of foliage moisten by intercepted rain evaporates at potential rate. In our study, this evaporation was accounted for in TR. In the ETR measurements, this term was generally not captured because the data were filtered during rain (or irrigation) events and during the following half hour (Béziat et al., 2009). Therefore, gap-filled ETR data are slightly underestimated as the gapfilling methods are constructed on rain free events. As the maximum annual simulated value for the evaporation of intercepted water was 17 mm at Lamasquère in 2006-07 (3.4 % of the annual simulated ETR), we assumed that this term did not significantly affect the cumulative water flux comparison for the two partitioning methods.

2.5. Water budget evaluation

The water budget was analyzed seasonally and annually using the following equation:

$$P\ (+I) - \Delta SWC = ETR + (D + R) \qquad (13)$$

where P is the precipitation measurement; I is irrigation provided by the farmer; ΔSWC is the integrated soil water content difference between the end and the beginning of the period; and D and R are the drainage and runoff terms, respectively. The P (+I) – ΔSWC term represents the available water for the ecosystem during the period considered. For this analysis, ΔSWC was integrated from the surface to a depth of 100 cm (ΔSWC_{0_100}) using the SWC profile measurements. The ETR + (D + R) term represents water lost from the ecosystem. The (D + R) term was calculated as the difference

between P (+I) – ΔSWC and the observed ETR. Therefore, (D + R) reflects both surface and deep water losses and uncertainties in the P (+I), ΔSWC and ETR measurements.

3. Results and discussion

3.1. Seasonal ETR and SWC dynamics

During the growing season, the ETR dynamics closely followed the LAI dynamics (Figure 2). For winter wheat crops, the maximal ETR (ETR_{max}) was observed in the middle of May, *i.e.*, at the beginning of senescence, whereas for the summer crops maize and sunflower, ETR_{max} was reached in the middle of July, corresponding to the LAI maximum (LAI_{max}). The delay in ETR_{max} compared to LAI_{max} observed for winter wheat crops may be explained by the seasonal dynamics of Rn, which reaches its maximum at the end of June. Therefore, ETR continuously increased after LAI_{max} was achieved. The vegetation then dried, and the Rn was preferentially dissipated through H, which increased following Rn.

The mean maximum ETR was 4.8 mm d^{-1} for winter wheat (ranging between 4.2 and 5.4 mm d^{-1}). The difference in the ETR_{max} observed between both winter wheat crops, favoring of the Lamasquère site, may be explained by the original LAI differences in the varietals or better development due to milder and wetter climatic conditions (Figure 2) (Tallec et al., submitted). For winter wheat, Steduto and Albrizio (2005) reported a similar ETR_{max} value (4.4 mm d^{-1}) to the one observed at our study sites and with a similar LAI_{max}. For summer crops, the mean maximum ETR values were 5.1 and 5.6 mm d^{-1} for sunflower and maize, respectively. Nevertheless, Suyker and Verma (2008) reported higher ETR_{max} values for summer crops, ranging between 6.5 and 8 mm d^{-1} for irrigated soybeans and maize, respectively. This difference in the ETR response can be explained by a lower LAI_{max} value of 3.3 m^2 m^{-2} for maize compared to the LAI values higher than 5.5 m^2 m^{-2} observed by Suyker and Verma (2008). The reduced maize development observed in our field was a consequence of less irrigation being used and differences in crop varieties and management practices, as explained in Béziat et al. (2009). Similarly for sunflower crops, Steduto and Albrizio (2005) and Karam et al. (2007) reported an ETR_{max} twice as high as that measured at Auradé over sunflower plots that were either irrigated or not, probably resulting from considerably higher LAI_{max} values (between 2.8 and 3.5 m^2 m^{-2} in Albrizio and Steduto (2005) and higher than 6 m^2 m^{-2} in Karam et al. (2007) compared to the value observed in the present study. However, when comparing the relative sunflower ETR response to that of other crops, the low LAI_{max} of 1.7 m^2 m^{-2} was not accompanied by a proportionally lower ETR_{max} as for other crops. This was probably caused by high stomatal conductance, which can be more than twice as high as that of maize (Katerji and Bethenod, 1997).

At Auradé, the integrated soil water content between 0 and 30 cm deep (SWC_{0_30}) (Figure 2c) decreased during winter wheat development because of low precipitation and root absorption. The

same pattern was observed for sunflower, but in this case, SWC_{0_30} began to decrease before the sunflower growing season, which was attributed to low precipitation associated with a Rn increase. We assumed that SWC_{0_30} decreased at Lamasquère during spring 2006 for the same reasons. During maize development, the effect of root absorption on SWC_{0_30} was strong, despite the irrigation employed. During spring 2007, the period of winter wheat development at Lamasquère coupled with the high precipitation level maintained higher SWC_{0_30} values compared to spring 2006. During senescence and after harvesting, low precipitation and high Rn increased ETR (corresponding to E) and caused the soil to dry. The absolute values of SWC_{0_30} were higher at Lamasquère than at Auradé because of two factors: 1) the greater water retention capacity of the soil due to higher clay content and 2) the proximity of the Touch River (about 400 m) inducing water rise in winter by capillarity up to the 0-30cm layer. Therefore, this absolute difference did not necessarily induce a difference in soil water availability for the plants.

During non-vegetation periods, ETR (corresponding to E) varied between 0 and 2 mm d^{-1}. This variation was explained in part by variations in Rn. In September 2006, the ETR_{max} was observed to be between 2.5 and 3 mm d^{-1} at both sites subsequent to important rainfall events (Figure 2c). The same phenomenon was observed at Lamasquère in March 2006 before maize sowing.

3.2. Comparison and evaluation of the performance of the partitioning methods

Statistical results comparing the ICARE-SVAT model output with the measurements are presented in Table 3. Overall, the different components of the energy budget were well reproduced by the model for both sites and both years. R^2 and Nash criterion values were close to 1, with mean respective R^2 and Nash values of 0.98 and 0.98 for Rn, 0.86 and 0.81 for LE and 0.76 and 0.70 for H being obtained. As expected, the model simulated Rn properly, with a mean slope of 1.00, a mean intercept of 0.97 W m^{-2} and an RMSE globally lower than 30 W m^{-2}. However, a small overestimation of Rn was observed at Auradé, especially in 2006-07 (mean bias equal to 5.67 W m^{-2} for both years), and a small underestimation was observed at Lamasquère, especially in 2005-06 (mean bias equal to -3.26 W m^{-2} for both years). With respect to Rn, a slight overestimation was observed for LE at Auradé (Figure 3), with a mean slope for this site of 1.09 and a mean bias of 3.68 W m^{-2} being observed. In contrast, at Lamasquère, the mean slope for LE was 0.99, and the mean bias was -2.28 W m^{-2}. However, the mean RMSE for LE at both sites and years was 30.17 W m^{-2}, which indicates that the model estimated LE correctly. H was slightly overestimated for both sites and both years, with a mean bias of 4.74 W m^{-2}. This H overestimation arose mostly after harvesting and before ploughing, indicating that the ICARE-SVAT model parameterization for stubble (height and albedo) might be inadequate. However, with an overall mean RMSE of 33.55 W m^{-2}, the H estimations performed by the ICARE-SVAT model were acceptable. The G estimations were less reliable, with a mean RMSE

of 42.52 W m^{-2} and low R^2 and Nash criterion values (0.68 and 0.29, respectively) being determined. Similar results are commonly produced by this kind of model (Olioso et al., 2002). The soil water content simulations integrated from the surface to 150 cm deep (SWC_{0_150}) obtained with ICARE-SVAT were highly accurate, with very low RMSE and mean bias values (both of about 1 %) and elevated R^2 and Nash criterion values (0.83 and 0.80, respectively). An exception to this was observed for Lamasquère in 2007 associated with irrigated maize, when less significant statistical values were obtained (see discussion below), but the ICARE-SVAT simulations were still acceptable. The simulation of the surface soil water content (SWC_{0_5}) was less accurate compare to the SWC_{0_150}, with a RMSE of 0.03 $m^3.m^{-3}$ and a mean Nash value of 0.14 but good R^2, slopes and bias. It could be explained by the use of the *force-restore* method for water transfer that forced the surface layer to follow the dynamic of the deep-water reservoir. Despite this problem, evaporation is correctly estimated on bare soil due to compensations introduced by surface resistance calibration.

Comparison of the ICARE-SVAT and MDS results with measurements performed during bare soil periods (Table 1) showed that E was estimated well by both methods (Table 4). The mean R^2 was 6 % higher, and the Nash criterion was 11 % higher for ICARE-SVAT than for MDS on average, showing a more scattered prediction for MDS. However, the mean slope was 13% higher, while the mean RMSE was 10% lower for MDS than for ICARE-SVAT. These results show that MDS allowed a realistic and non-biased estimation of E during bare soil periods. Moreover, the estimations of TR produced by MDS and ICARE-SVAT were very similar, with a mean slope for both sites and years of 0.99, a mean RMSE of 0.02 g H_2O m^{-2} s^{-1}, a mean R^2 of 0.79 and a Nash criterion value of 0.72.

The cumulative E dynamics estimated by MDS (E_{MDS}) and ICARE-SVAT (E_{ICARE}) were in good agreement (Figure 3). In June 2006, at the end of winter wheat development at Auradé, drying of the surface evaporative layer induced high soil resistance to E (Equation 9), which led to lower values of accumulated E_{ICARE} compared to E_{MDS}. For winter wheat at Lamasquère in 2007, E_{ICARE} was lower than E_{MDS} because of the impact of dew simulated by the model (negative E values). In the ICARE-SVAT model, this phenomenon appeared in May 2007, corresponding to a period of colder temperatures, high precipitation and elevated soil water content (Figure 2). Although this phenomenon is plausible, its importance seemed to be too high, as confirmed by the slight underestimation of ETR by ICARE-SVAT. Both the phenomena of excessive drying and dew formation could be explained by the "force-restore" water and temperature dynamics (Gentine et al. 2007, 2011). This soil representation induces strong water exchange between the evaporative surface layer and the root absorption layer. During periods without precipitation the soil surface layer drying resulted in a significantly reduced E, as observed for Auradé winter wheat. For winter wheat at Lamasquère, because of the high precipitation during spring 2007, the modeled surface evaporative layer was always water saturated. This induced low soil surface temperatures (the mean daily modeled soil surface temperatures were 1.7 °C lower on average than the temperature measured 10 cm deep

between April and June 2007) and dew deposition instead of E (31% of E_{ICARE} data were negative between April and June 2007). The difference between the E estimations from ICARE-SVAT and MDS at Auradé in 2007 corresponds to an overestimation of ETR by ICARE-SVAT compared to the observed ETR, which arose before the full development of the crop and before high TR values were observed. Therefore, the overestimation of Rn by ICARE-SVAT noted above (see Table 3) was probably the main cause of the overestimation of ETR and E by ICARE-SVAT compared to the observed values and to E_{MDS}.

On both a seasonal and annual basis, the ICARE-SVAT and MDS partitioning between E and TR were quite comparable (Table 6). The mean absolute difference between the E estimation methods was 24 mm on the seasonal time scale and 30 mm on the annual time scale. These differences can be considered to represent an estimation of the uncertainty of the MDS method. The greater differences observed for winter wheat at Auradé and Lamasquère were the result of particular meteorological conditions and phenomena that the ICARE-SVAT simulation failed to describe, as explained above. However, this did not induce an additional systematic error in MDS partitioning, even though such an error could have been introduced, as both methods were calibrated during bare soil periods and applied during vegetation periods. Radiative transfer, soil temperature and SWC dynamics were taken into account in both cases, but differences in soil texture induced by tillage and progressive ground collapse between sowing and harvesting were not considered. Soil properties and E might have been impacted by these changes.

Additional and more comprehensive analyses of the uncertainties and processes involved in these two partitioning methods would require accurate separate measurements of E and TR, which are currently almost impossible. Sap flow measurements only represent one plant and the magnitude of the flow can hardly be compared to the total transpiration. In addition sap flow measurements can be delayed because of the internal water storage within the plant (Goldstein et al. 1998).

3.3. Water budget distribution, component dynamics and drivers

Mean annual precipitation is 615 mm at Lamasquère and 684 mm at Auradé (Table 5). Precipitation was low during maize development, which was partly compensated for by irrigation. Negative and positive values of ΔSWC_{0_100} were observed, representing soil water reserve increases and decreases, respectively, during the considered period.

ETR represented 78 % of the available water P (+I) – ΔSWC; (see Equation 13) on average on annual time scale. On seasonal time scale, ETR was very similar for all crops, with absolute values ranging between 350 and 400 mm. ETR represented 76% of available water during the growing season for winter wheat, 81% for sunflower and 105% for maize on average. This difference between winter and summer crops was the result of lower water inputs for summer crops than for winter crops during

their respective growing seasons, even when considering irrigation. Rn was also higher during summer, which led to higher potential evaporative demands and water absorption by the plant cover. For winter wheat, the seasonal ETR was comparable to that reported by Qiu et al. (2008), ranging between 257.3 and 467.5 mm depending on the irrigation supply. In a study performed by Suyker and Verma (2009), higher ETR values were observed for summer crops on a seasonal time scale, ranging between 431 mm for rainfed soybeans to 548 mm for irrigated maize. These higher values resulted from higher water inputs and higher LAI values for their crops.

Although the amounts of annual precipitation are higher at Auradé, estimations of drainage plus runoff water losses represented 26% of the apparent annual water availability, compared to only 18% at Lamasquère (Figure 4a). This higher value at Auradé is consistent with the slight slope of this site. The slop might have increased the runoff term during high precipitation events compared to Lamasquère. On seasonal time scale, D + R was important for winter wheat at Lamasquère (Figure 4b) because of the high precipitation on saturated soil in the spring (Figure 2). The negative value of D + R for maize at Lamasquère is an artifact that illustrates the measurement uncertainties for P, ΔSWC_{0_100} and ETR. It therefore represents a negligible value for water loss through drainage and runoff.

Overall, based on annual and seasonal time scales, the absolute values of E and its contribution to ETR were higher at Auradé than at Lamasquère (Figure 4 and Table 5). These results were attributed to the higher accumulated incoming radiation at the soil surface layer at Auradé. Indeed, low LAI values (especially for sunflower, see Table 6) coupled to longer bare soil periods (338 days for Auradé *versus* 277 days for Lamasquère for both years) led to higher RG_s values (see section 2.2) at the Auradé site. The differences in the proportion of E in ETR between the seasonal and annual time scales (Figure 4) were more pronounced for maize because of the longer bare soil periods (the regrowth period observed at Lamasquère at the end of 2005 was excluded from the bare soil periods). In contrast, as expected, the absolute values of TR and its contribution to ETR were always higher at Lamasquère. The lower LAI values for Auradé winter wheat and sunflower compared to Lamasquère winter wheat and maize might also explain the lower TR values for Auradé. Moreover, maize irrigation increased the water input and the water available for TR. On annual time scale, according to site management, longer bare soil periods for summer crops explained the lower proportion of TR in the annual ETR compared to winter wheat. The highest proportion of TR in annual ETR was observed for winter wheat at Lamasquère (48%). Indeed, an exceptionally warm winter (Béziat et al., 2009) caused high LAI values, even early in the growing season (Figure 2), and these values remained higher than 1 m^2 m^{-2} from January to June 2007.

In conclusion, the partitioning of ETR between E and TR during vegetation periods was mainly driven by incoming radiation partitioning between soil and vegetation, which directly depends on vegetation density and LAI. The partitioning is primarily driven by the duration of the bare soil period on annual time scale and by the LAI crop development dynamics during growing seasons at

both seasonal and annual time scales. This last observation is consistent with the results of a study performed on grasslands reported by Hu et al. (2009), who showed that the ratio of annual E/ETR increased from 51% to 67% with a decrease in the mean LAI from 1.9 to 0.5 m^2 m^{-2}.

4. Conclusions

Eddy-covariance allow investigating of long-term dynamics of ETR yet do not directly discriminate between the soil E and vegetation TR contributions. A marginal distribution sampling (MDS) method is here used based on few field data to partition, total ETR in E and TR. MDS results were compared to simulations of the site-calibrated ICARE-SVAT double-source mechanistic model. Both methods showed a consistent ETR partitioning. The great advantage of the MDS method is that it does not require calibration and has very few parameters. Reductionism can help fundamentally improve our understanding of the physical processes and our predictive power, as long as it does not try to oversimplify the physics but attempts at capturing the observed emergent behavior of the physical system (Sivapalan 2003). The MDS method aims at capturing the main processes behind the ETR partitioning. Complex land-surface models insufficiently calibrated against short-term measurements can observe the right ETR over a few days yet along with wrong soil-vegetation water flux partitioning: the right answer for the wrong reasons.

With partitioning method, we showed that the water budget partitioning between the different components strongly depends on crop plot management and climate variability. E was shown to represent nearly one-third of the water budget during the growing season and nearly half of the water budget on annual time scale. Consequently changes in agricultural practices should help better mitigate soil water use and improve production efficiency. For instance, water losses through E can be mitigated by reducing the bare soil period and by promoting mulching, intercrop or cover crops. This study has focused on water use yet has not considered other components essential to plant growth such as nutrients. Use of intercrop or cover crops should be carefully considered as they would increase TR and could limit the development of the subsequent crop due to mobilizing available nitrogen. The effect of nutrients will be evaluated in future work.

Acknowledgements

This work was made possible through the support of the European Commission (FEDER Interreg IVa program, ref POCTEFA 08/34), the French Ministry in Charge of Research ("Réseau Terre et Espace"), the Ministry in Charge of Environment (GICC programme), the Centre National de la Recherche Scientifique (CNRS), the Institut National des Sciences de l'Univers (INSU), the Centre National d'Etudes Spatiales (CNES) and the Région Midi-Pyrénées Council. We are very grateful to Mr. Andréoni (farmer) and to Michel Gay, Jean-Paul Kummel and Benoît Cantaloube from the Ecole Supérieure d'Agriculture de Purpan for accommodating our measurement devices in their respective fields at Auradé and Lamasquère. We wish to thank the reviewers for helping us improving this paper. Special thanks to our technical staff: Nicole Ferroni, Hervé Gibrin, Pascal Keravec and Bernard Marciel. We also have a sweet thought for Pierre who passed away in July 2010. He was at the origin of this paper that we dedicate to his parents, Monique and Francis, and to his fiancée Elodie.

References

Allen, R.G., 2008. Quality assessment of weather data and micrometeorological flux: impacts on evapotranspiration calculation. J. Appl. Meteorol., 64(4): 191-204.

Albrizio, R. and Steduto, P., 2005. Resource use efficiency of field-grown sunflower, sorghum, wheat and chickpea: I. Radiation use efficiency. Agric. For. Meteorol., 130(3-4): 254-268.

Aubinet, M., Grelle, A., Ibrom, A., Rannik, U., Moncrieff, J., Foken, T., Kowalski, A.S., Martin, P.H., Berbigier, P., Bernhofer, C., Clement, R., Elbers, J., Granier, A., Grun-wald, T., Morgenstern, K., Pilegaard, K., Rebmann, C., Snijders, W., Valentini, R., Vesala, T., 2000. Estimates of the annual net carbon and water exchange of forests: the EUROFLUX methodology. Adv. Ecol. Res. 30, 113–175

Baldocchi, D.D., 2003. Assessing the eddy covariance technique for evaluating carbon dioxide exchange rates of ecosystems: past, present and future. Global Change Biol., 9: 479-492.

Beven, K., 2006. A manifesto for the equifinality thesis. J. Hydrol., 320(1-2): 18-36.

Béziat, P., Ceschia, E. and Dedieu, G., 2009. Carbon balance of a three crop succession over two cropland sites in South West France. Agric. For. Meteorol., 149(10): 1628-1645.

Boulet, G., Chehbouni, A., Braud, I. and Vauclin, M., 1999. Mosaic versus dual source approaches for modelling the surface energy balance of a semi-arid land. Hydrol. Earth Syst. Sci., 3(2): 247-258.

Braud, I., Dantas-Antonino, A.C., Vauclin, M., Thony, J.L. and Ruelle, P., 1995. A simple soil-plant-atmosphere transfer model (SiSPAT) development and field verification. J. Hydrol., 166(3-4): 213-250.

Brouder, S.M. and Volenec, J.J., 2008. Impact of climate change on crop nutrient and water use efficiencies. Physiol. Plant., 133(4): 705-724.

Brutsaert, W., 1982. Evaporation Into the Atmosphere, D. Reidel, Hingham, Mass, 299 pp.

Chen, F., Mitchell, K., Schaake, J., Xue, Y., Pan, H.-L., Koren, V., Duan, Q.Y., Ek, M. and Betts, A., 1996. Modeling of land surface evaporation by four schemes and comparison with FIFE observations. J. Geophys. Res., 101.

Choudhury, B.J. and Monteith, J.L., 1988. A four-layer model for the heat budget of homogeneous land surfaces. Q. J. Royal Meteorol. Soc., 114(480): 373-398.

Deardorff, J.W., 1977. A parameterization of ground surface moisture content for use in atmospheric prediction models. J. Appl. Meteorol., 16: 1182-1185.

Deardorff, J.W., 1978. Efficient prediction of ground surface temperature and moisture with inclusion of a layer of vegetation. J. Geophys. Res., 20, 1889-1903.

570 Demarez, V., Duthoit, S., Baret, F., Weiss, M. and Dedieu, G., 2008. Estimation of leaf area and
571 clumping indexes of crops with hemispherical photographs. Agric. For. Meteorol., 148(4):
572 644-655.
573 Dickinson, R. E., 1984. Modeling evapotranspiration for three dimensional global climate models.
574 Climate Processes and Climate Sensitivity. Geophys. Monogr., 29, 58-72.
575 Dolman, A.J., Noilhan, J., Durand, P., Sarrat, C., Brut, A., Piguet, B., Butet, A., Jarosz, N., Brunet, Y.,
576 Loustau, D., Lamaud, E., Tolk, L., Ronda, R., Miglietta, F., Gioli, B., Magliulo, V., Esposito,
577 M., Gerbig, C., rner, S., Glademard, P., Ramonet, M., Ciais, P., Neininger, B., Hutjes,
578 R.W.A., Elbers, J.A., Macatangay, R., Schrems, O., rez-Landa, G., Sanz, M.J., Scholz, Y.,
579 Facon, G., Ceschia, E. and Béziat, P., 2006. The CarboEurope Regional Experiment Strategy.
580 Bulletin of the American Meteorological Society, 87(10): 1367-1379.
581 Gentine, P., Entekhabi, D., Chehbouni, A., Boulet, G. and Duchemin, B., 2007. Analysis of
582 evaporative fraction diurnal behaviour. Agric. For. Meteorol., 143(1-2): 13-29.
583 Gentine P., Polcher J. and Entekhabi D., 2011. Harmonic propagation of variability in surface energy
584 balance within a coupled soil-atmosphere system, Water Resources Research, (47) W05525,
585 21, doi:10.1029/2010WR009268
586 Goldstein, G., Andrade, J., Meinzer, F., Holbrook, N., Cavelier, J., Jackson, P., & Celis, A. (1998).
587 Stem water storage and diurnal patterns of water use in tropical forest canopy trees. Plant Cell
588 And Environ., *21*(4), 397–406.
589 Goudriaan, J., 1977. Crop micrometeorology: a simulation study, Wageningen, The Netherlands,
590 249pp pp.
591 Granier, A., Biron, P., Bréda, N., Pontailler, J.-Y. and Saugier, B., 1996. Transpiration of trees and
592 forest stands: short and long-term monitoring using sapflow methods. Global Change Biol.,
593 2(3): 265-274.
594 Grelle, A. and Lindroth, A., 1996. Eddy-correlation system for long-term monitoring of fluxes of heat,
595 water vapour and CO_2. Global Change Biol., 2: 297-307.
596 Hartmann, D.L., 1994. Global Physical Climatology, Hardbound, 411 pp.
597 Hu, Z., Yu, G., Zhou, Y., Sun, X., Li, Y., Shi, P., Wang, Y., Song, X., Zheng, Z., Zhang, L. and Li, S.,
598 2009. Partitioning of evapotranspiration and its controls in four grassland ecosystems:
599 Application of a two-source model. Agricultural and Forest Meteorology, 149(9): 1410-1420.
600 IPCC, 2007. Climate Change 2007: Synthesis Report. Contribution of Working Groups I, II and III to
601 the Fourth Assessment Report of the Intergovernmental Panel on Climate Change. IPCC,
602 Geneva, Switzerland, 104 pp.
603 Jarosz, N., Brunet, Y., Lamaud, E., Irvine, M., Bonnefond, J.-M. and Loustau, D., 2008. Carbon
604 dioxide and energy flux partitioning between the understorey and the overstorey of a maritime
605 pine forest during a year with reduced soil availability Agricultural and Forest Meteorology,
606 148: 1508-1523.

607 Jarvis, P.G., 1976. The interpretation of the variations in leaf water potential and stomatal conductance
608 found in canopies in the field. Phil. Trans. Roy. Soc. London, B273: 593-610.
609 Karam, F., Lahoud, R., Masaad, R., Kabalan, R., Breidi, J., Chalita, C. and Rouphael, Y., 2007.
610 Evapotranspiration, seed yield and water use efficiency of drip irrigated sunflower under full
611 and deficit irrigation conditions. Agricultural Water Management, 90(3): 213-223.
612 Katerji, N. and Bethenod, O., 1997. Comparaison du comportement hydrique et de la capacité
613 photosynthétique du maïs et du tournesol en condition de contrainte hydrique. Conclusions sur
614 l'efficience de l'eau. Agronomie, 17(1): 17-24.
615 Kersteins, G., 1996. Cuticular water permeability and its physiological significance. J. Exp. Bot.,
616 47(305): 1813-1832.
617 Koren, V., Schaake, J., Mitchell, K., Duan, Q.Y., Chen, F. and Baker, J.M., 1999. A parameterization
618 of snowpack and frozen ground intended for NCEP weather and climate models. J. Geophys.
619 Res., 104.
620 Lamaud, E., Brunet, Y. and Berbigier, P., 1996. Radiation and water use efficiencies of two coniferous
621 forest canopies. Phys. Chem. Earth, 21(5-6): 361-365.
622 Li, Q., Chen, Y., Liu, M., Zhou, X., Yu, S. and Dong, B., 2008. Effects of Irrigation and Straw
623 Mulching on Microclimate Characteristics and Water Use Efficiency of Winter Wheat in
624 North China. Plant Production Science, 11(2): 161-170.
625 Medrano, H., Flexas, J. and Galmés, J., 2009. Variability in water use efficiency at the leaf level
626 among Mediterranean plants with different growth forms. Plant Soil, 317(1): 17-29.
627 Moncrieff, J.B., Massheder, J.M., de Bruin, H., Elbers, J., Friborg, T., Heusinkveld, B., Kabat, P.,
628 Scott, S., Soegaard, H. and Verhoef, A., 1997. A system to measure surface fluxes of
629 momentum, sensible heat, water vapour and carbon dioxide. Journal of Hydrology, 188-189:
630 589-611.
631 Moore, C.J., 1986. Frequency response corrections for eddy correlation systems. Boundary-Layer
632 Meteorol., 37(1 - 2): 17-35.
633 Nash, J.E. and Sutcliffe, J.V., 1970. River flow forecasting through conceptual models part I -- A
634 discussion of principles. J. Hydrol., 10(3): 282-290.
635 Noilhan, J. and Mahfouf, J.F., 1996. The ISBA land surface parameterization scheme. Global Planet.
636 Change, 13: 145-159.
637 Noilhan, J. and Planton, S., 1989. A simple parameterisation of land surface processes for
638 meteorological models. Monthly Weather Rev., 117: 536-549.
639 Ogée, J., Brunet, Y., Loustau, D., Berbigier, P. and Delzon, S., 2003. MuSICA, a CO_2, water and
640 energy multilayer, multileaf pine forest model: evaluation from hourly to yearly time scales
641 and sensitivity analysis. Global Change Biol., 9(5): 697-717.
642 Olioso, A., Braud, I., Chanzy, A., Courault, D., Demarty, J., Kergoat, L., Lewan, E., Ottléc, C., Prévot,
643 L., Zhao, W.G., Calvet, J.-C., Cayrol, P., Jongschaap, R., Moulin, S., Noilhan, J. and

Wigneron, J.-P., 2002. SVAT modeling over the Alpilles-ReSeDA experiment: comparing SVAT models over wheat fields. Agronomie, 22(6): 651-668.

Passerat De Silans, A., Bruckler, L., Thony, J.L. and Vauclin, M., 1989. Numerical modeling of coupled heat and water flows during drying in a stratified bare soil -- Comparison with field observations. J. Hydrol., 105(1-2): 109-138.

Qiu, G.Y., Wang, L., He, X., Zhang, X., Chen, S., Chen, J. and Yang, Y., 2008. Water use efficiency and evapotranspiration of winter wheat and its response to irrigation regime in the north China plain. Agricultural and Forest Meteorology, 148(11): 1848-1859.

Reichstein, M., Falge, E., Baldocchi, D., Papale, D., Aubinet, M., Berbigier, P., Bernhofer, C., Buchmann, N., Gilmanov, T., Granier, A., Grunwald, T., Havrankova, K., Ilvesniemi, H., Janous, D., Knohl, A., Laurila, T., Lohila, A., Loustau, D., Matteucci, G., Meyers, T., Miglietta, F., Ourcival, J.-M., Pumpanen, J., Rambal, S., Rotenberg, E., Sanz, M., Tenhunen, J., Seufert, G., Vaccari, F., Vesala, T., Yakir, D. and Valentini, R., 2005. On the separation of net ecosystem exchange into assimilation and ecosystem respiration: review and improved algorithm. Global Change Biology, 11(9): 1424-1439.

Ritchie, J.T., 1972. Model for Predicting Evaporation from a Row Crop with incomplete Cover. Water Resour. Res., 8(5): 1204-1213.

Roupsard, O., Bonnefond, J.-M., Irvine, M., Berbigier, P., Nouvellon, Y., Dauzat, J., Taga, S., Hamel, O., Jourdan, C., Saint-André, L., Mialet-Serra, I., Labouisse, J.-P., Epron, D., Joffre, R., Braconnier, S., Rouzière, A., Navarro, M. and Bouillet, J.-P., 2006. Partitioning energy and evapo-transpiration above and below a tropical palm canopy. Agricultural and Forest Meteorology, 139(3-4): 252-268.

Sauer, T.J., Singer, J.W., Prueger, J.H., DeSutter, T.M. and Hatfield, J.L., 2007. Radiation balance and evaporation partitioning in a narrow-row soybean canopy. Agric. For. Meteorol., 145(3-4): 206-214.

Sellers, P.J., Randall, D.A., Collatz, G.J., Berry, J.A., Field, C.B., Dazlich, D.A., Zhang, C., Collelo, G.D. and Bounoua, L., 1996. A Revised Land Surface Parameterization (SiB2) for Atmospheric GCMS. Part I: Model Formulation. Journal of Climate, 9(4): 676-705.

Shuttleworth, W.J. and Wallace, J.S., 1985. Evaporation from sparse crops-an energy combination theory. Q. J. Royal Meteorol. Soc., 111(469): 839-855.

Sivapalan, M. (2003). Prediction in ungauged basins: a grand challenge for theoretical hydrology. Hydrological Processes, *17*(15), 3163–3170. doi:10.1002/hyp.5155

Steduto, P. and Albrizio, R., 2005. Resource use efficiency of field-grown sunflower, sorghum, wheat and chickpea: II. Water use efficiency and comparison with radiation use efficiency. Agric. For. Meteorol., 130(3-4): 269-281.

679 Steduto, P., Katerji, N., Puertos-Molina, H., U¨nlu¨, M., Mastrorilli, M. and Rana, G., 1997. Water-use
680 efficiency of sweet sorghum under water stress conditions Gas-exchange investigations at leaf
681 and canopy scales. Field Crops Research, 54(2-3): 221-234.
682 Steiner, J.L. and Hatfield, J.L., 2008. Winds of Change: A Century of Agroclimate Research. Agron J,
683 100(Supplement_3): S-132-152.
684 Steppe, K., De Pauw, D.J.W. Doody T.M. and Teskey R.O., 2010. A comparison of sap flux density
685 using thermal dissipation, heat pulse velocity and heat field deformation methods, Agric. For.
686 Meteorol., 150 (7–8): 1046–1056.
687 Suyker, A.E. and Verma, S.B., 2008. Interannual water vapor and energy exchange in an irrigated
688 maize-based agroecosystem. Agric. For. Meteorol., 148(3): 417-427.
689 Suyker, A.E. and Verma, S.B., 2009. Evapotranspiration of irrigated and rainfed maize-soybean
690 cropping systems. Agric. For. Meteorol., 149(3-4): 443-452.
691 Taconet, O., Bernard, R. and Vidal-Madjar, N., 1986. Evapotranspiration over an agricultural region
692 using a surface flux/temperature model based on NOAA-AVHRR data. J. Clim. Appl.
693 Meteorol., 25: 284-307.
694 Webb, E.K., Pearman, G.I. and Leuning, R., 1980. Correction of flux measurement for density effects
695 due to heat and water vapour transfer. Quart. J. Met. Soc., 106: 85-100.
696 Williams, D.G., Cable, W., Hultine, K., Hoedjes, J.C.B., Yepez, E.A., Simonneaux, V., Er-Raki, S.,
697 Boulet, G., de Bruin, H.A.R., Chehbouni, A., Hartogensis, O.K. and Timouk, F., 2004.
698 Evapotranspiration components determined by stable isotope, sap flow and eddy covariance
699 techniques. Agricultural and Forest Meteorology, 125(3-4): 241-258.

Figures Captions

Figure 1: Schematic representation of energy partitioning with the ICARE model. λETR is the latent heat flux (evapotranspiration) composed of λTR (transpiration) from vegetation and λE (evaporation) from soil.

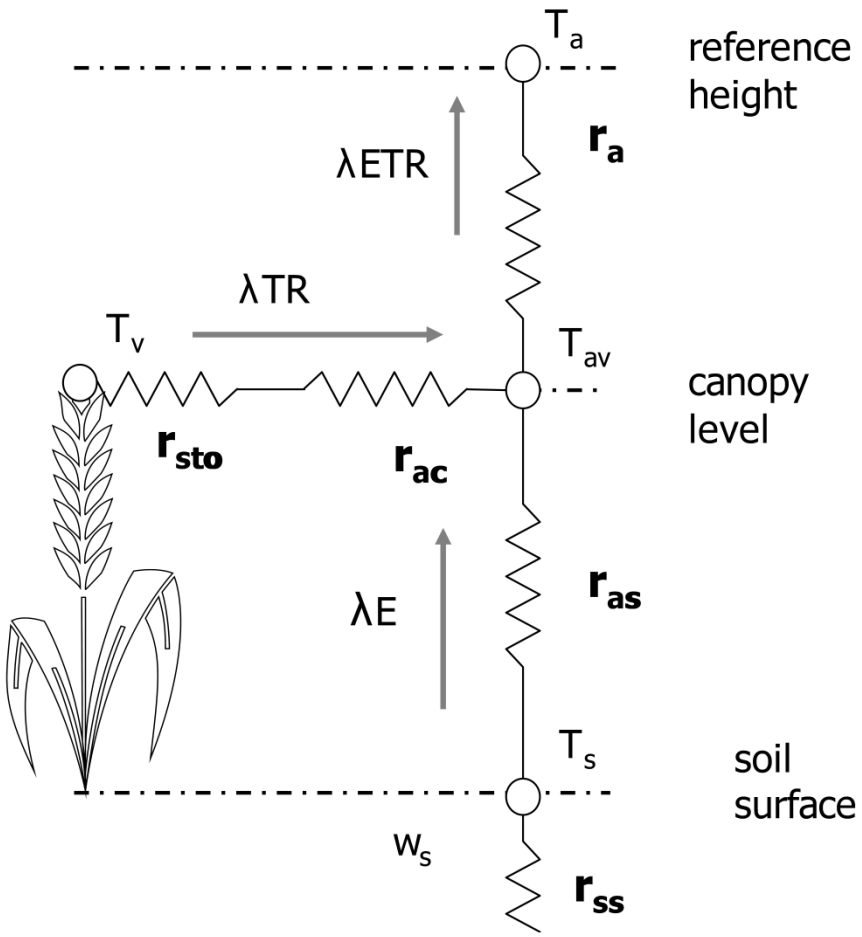

Figure 2: Seasonal dynamics of the daily evapotranspiration (ETR), net radiation (R_n) and sensible heat flux (H) at Auradé (a) and Lamasquère (b). (c) Daily soil water content between 0 and 30 cm deep (SWC_{0_30}, open and full circles), daily precipitation at both sites and irrigation at Lamasquère (P, solid and dotted lines and I, gray bars, respectively). (d) Observed leaf area index (LAI, open and full circles) and interpolated LAI (solid and dotted lines) from October 2005 to October 2007. In (d), the error bars correspond to ± one standard deviation of the mean.

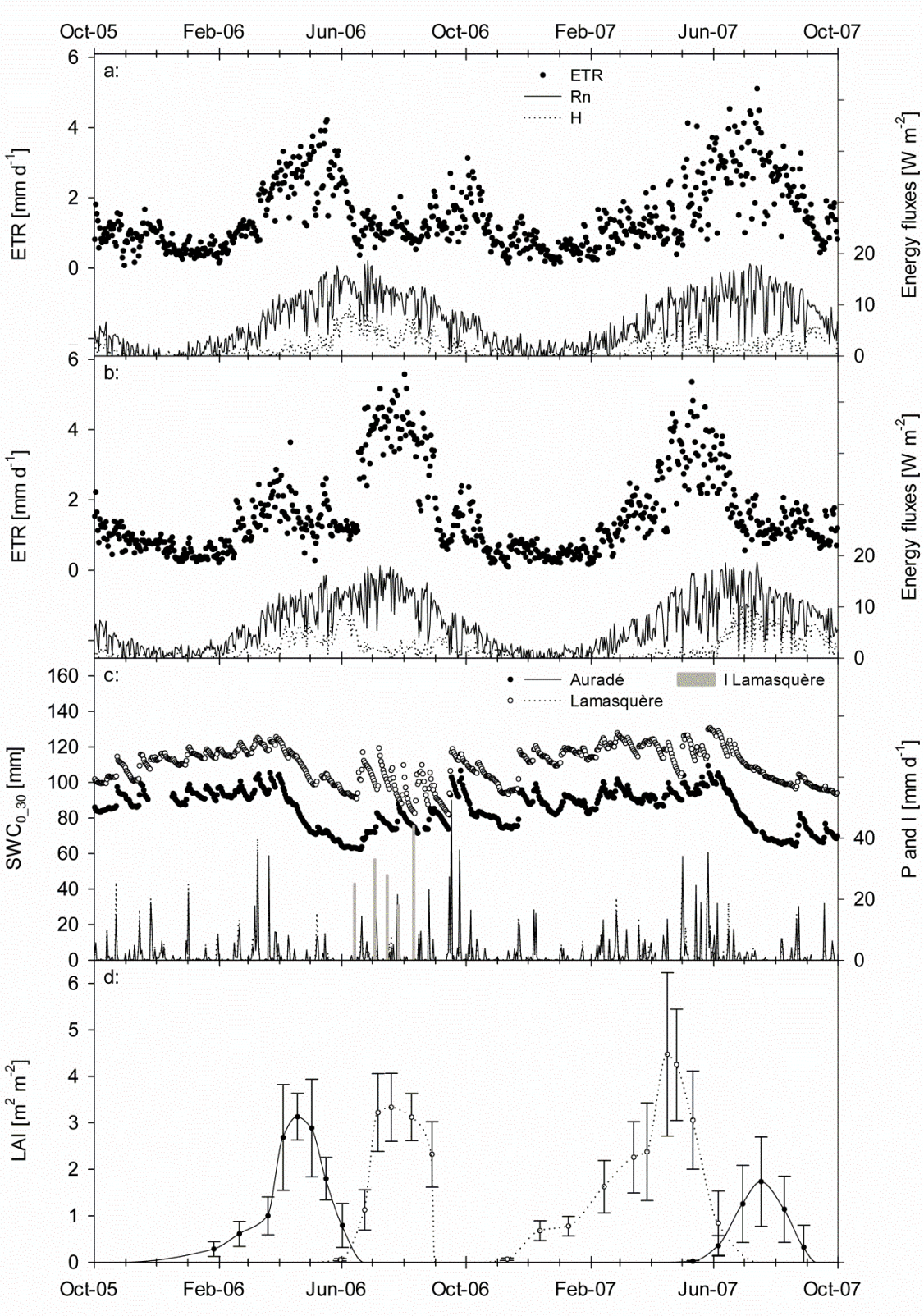

Figure 3: Comparison of cumulative evapotranspiration (ETR) measured by EC (ETR_{OBS}) and simulated with the ICARE-SVAT model (ETR_{ICARE}) and soil evaporation (E) calculated with the marginal distribution sampling method (E_{MDS}) and with the ICARE-SVAT model (E_{ICARE}) for both sites and both years. Annotations indicate dates of sowing (s), harvesting (h) and ploughing (p) and the name of the crop (or regrowth event).

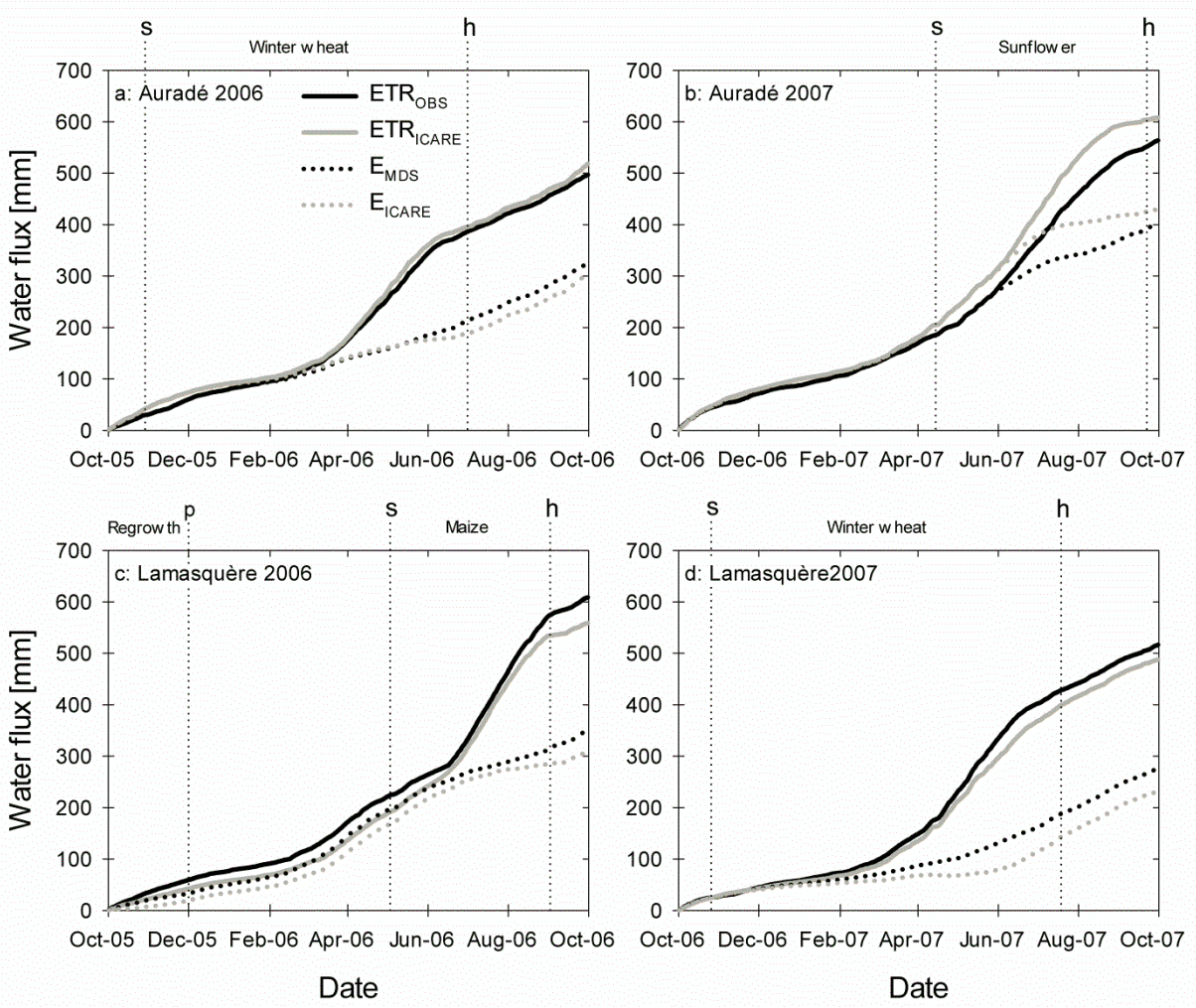

Figure 4: Estimation of the seasonal and annual contribution of transpiration (Tr), evaporation (E) and drainage + runoff (D + R) to water losses at the Auradé and Lamasquère sites.

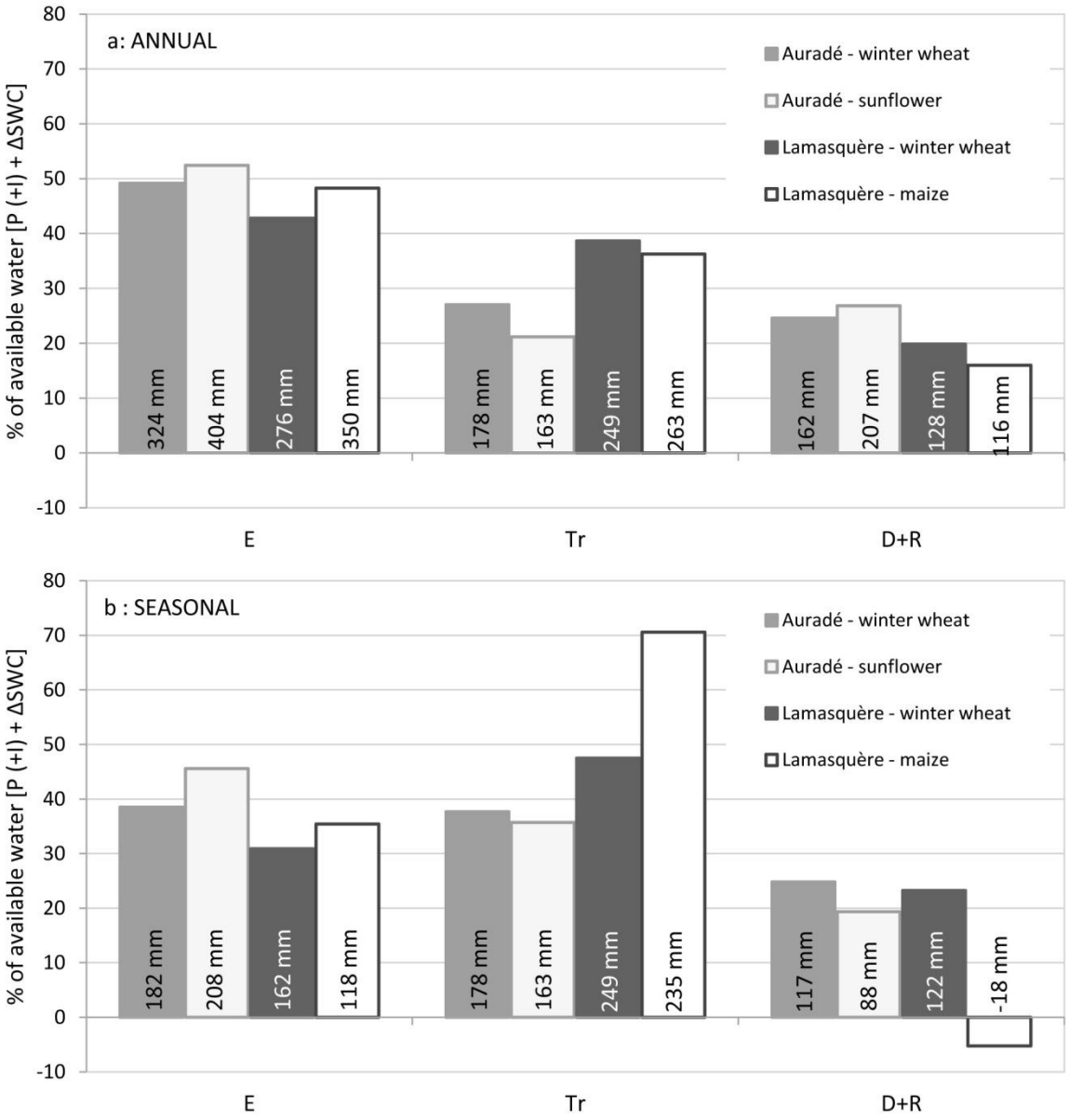

Table 1: Bare soil periods and corresponding number of available filtered half-hourly evapotranspiration (ETR) measurements.

Site	Start date	Technical operation	End date	Event/ technical operation	Number of ETR measurements
Auradé	4 July 2005	disking	8 July 2005	re-growth	150
	4 August 2005	disking	28 August 2005	re-growth	889
	23 September 2005	ploughing	27 October 2005	Winter wheat seeding	1192
	30 September 2006	ploughing	10 April 2007	sunflower seeding	5571
	20 September 2007	ploughing	1st October 2007	end of the dataset	305
					8107 (total)
Lamasquère	11 July 2005	disking	27 August 2005	re-growth	1780
	1st December 2005	ploughing	1st May 2006	maize seeding	4137
	31 August 2006	disking	18 October 2006	Winter wheat seeding	1268
					7185 (total)

Table 2: Best fit parameters from the ICARE-SVAT model resistance optimisation (see text for details) for Auradé and Lamasquère and for each crop. Global simulation parameters and bare soil parameters for the comparison with the marginal distribution sampling method are reported.

	Auradé		Lamasquère	
Parameter	Winter wheat	Sunflowers	Maize	Winter wheat
$A_{rss\ (global)}$ [ln(s m^{-1})]	21		38	
$Z_0/Z_{0h\ (global)}$ [dimensionless]	5		37*	
$A_{rss\ (bare\ soil)}$ [ln(s m^{-1})]	20		43	
$Z_0/Z_{0h\ (bare\ soil)}$ [dimensionless]	6		65*	
SWC_{wilt} [m^3 m^{-3}]	0.08	0.08	0.08	0.2
r_{smin} [s m^{-1}]	75	66	130	48

** Z_0/Z_{0h} values obtained for Lamasquère site are high values according to literature, but are resulting of a global optimization process with an absolute minimum convergence.*

Table 3: ICARE-SVAT model evaluation for energy budget variables (net radiation (Rn), latent heat flux (LE), sensible heat flux (H) and soil heat flux (G)) and for surface and deep soil water content (SWC_{0_5}, SWC_{0_150}) integrated over 0 to 5 and 0 to 150 cm down.

	Slope	Intercept	R^2	RMSE	Mean bias	Nash	n
Auradé							
2005-2006							
Rn [W m^{-2}]	0.99	2.97	0.97	31.52	2.19	0.97	15535
LE [W m^{-2}]	1.11	-2.36	0.88	26.78	2.73	0.82	10948
H [W m^{-2}]	0.86	7.27	0.77	36.36	3.77	0.76	12733
G [W m^{-2}]	1.13	3.07	0.63	45.43	3.20	0.24	15707
$SWC_{0\ 5}$ [m^3 m^{-3}]	0.85	0.06	0.68	0.03	0.02	0.39	15706
$SWC_{0\ 150}$ [m^3 m^{-3}]	0.86	0.04	0.92	0.01	0.00	0.92	15707
2006-2007							
Rn [W m^{-2}]	1.04	6.87	0.98	26.00	9.15	0.98	15936
LE [W m^{-2}]	1.08	0.77	0.80	37.91	4.64	0.70	11164
H [W m^{-2}]	0.98	8.16	0.66	38.02	7.91	0.48	12776
G [W m^{-2}]	1.00	0.63	0.68	36.29	0.63	0.54	17161
$SWC_{0\ 5}$ [m^3 m^{-3}]	0.74	0.10	0.54	0.05	0.04	0.00	17211
$SWC_{0\ 150}$ [m^3 m^{-3}]	0.89	0.03	0.85	0.01	0.00	0.85	17161
Lamasquère							
2005-2006							
Rn [W m^{-2}]	1.00	-7.20	0.99	19.11	-7.37	0.99	16739
LE [W m^{-2}]	0.96	-1.26	0.88	29.34	-3.74	0.87	10250
H [W m^{-2}]	0.69	10.81	0.75	29.24	4.29	0.74	11809
G [W m^{-2}]	1.24	-0.29	0.70	49.62	0.16	0.28	17151
$SWC_{0\ 5}$ [m^3 m^{-3}]	0.46	0.21	0.71	0.03	0.02	0.21	17150
$SWC_{0\ 150}$ [m^3 m^{-3}]	0.94	0.03	0.72	0.02	0.00	0.64	17151
2006-2007							
Rn [W m^{-2}]	0.99	1.25	0.97	25.78	0.84	0.97	17118
LE [W m^{-2}]	1.01	-1.56	0.88	26.67	-0.82	0.86	11567
H [W m^{-2}]	0.71	10.93	0.85	30.59	2.98	0.83	13397
G [W m^{-2}]	1.37	8.83	0.72	38.73	6.84	0.11	17409
$SWC_{0\ 5}$ [m^3 m^{-3}]	0.62	0.26	0.29	0.04	0.02	0.13	17459
SWC_{0_150} [m^3 m^{-3}]	0.61	0.16	0.66	0.01	0.01	0.50	17409

Table 4: Comparison of ETR measurements during bare soil periods with soil evaporation (E) prediction of the marginal distribution sampling method (MDS) and of the ICARE-SVAT model and comparison of transpiration (TR) estimated by both approaches over both years of experiment. Bare soil corresponds to the validation bare soil dataset (see section 2.4).

	Dataset	Slope	Intercept g H_2O m^{-2} s^{-1}	R^2	RMSE g H_2O m^{-2} s^{-1}	Mean bias g H_2O m^{-2} s^{-1}	Nash	n
Auradé								
E_{ICARE} vs. ETR	bare soil validation	0.71	0.003	0.76	0.012	-0.0020	0.75	3412
E_{MDS} vs. ETR	bare soil validation	0.97	-0.001	0.66	0.012	-0.0018	0.50	3395
TR_{ICARE} vs. TR_{MDS}	2005-2006	1.16	-0.001	0.84	0.014	0.0033	0.71	3681
TR_{ICARE} vs. TR_{MDS}	2006-2007	0.88	0.006	0.64	0.019	0.0019	0.55	2730
Lamasquère								
E_{ICARE} vs. ETR	bare soil validation	1.03	0.005	0.74	0.012	0.0050	0.54	2707
E_{MDS} vs. ETR	bare soil validation	1.03	-0.002	0.76	0.010	-0.0011	0.67	2679
TR_{ICARE} vs. TR_{MDS}	2005-2006	0.88	0.002	0.82	0.018	-0.0027	0.81	3628
TR_{ICARE} vs. TR_{MDS}	2006-2007	1.04	0.000	0.84	0.015	0.0011	0.80	4708

Table 5: Seasonal and annual cumulative values of precipitation and irrigation (P + (I)), soil water content variation integrated over 0 to 100 cm deep (ΔSWC_{0_100}), evapotranspiration observations (ETR_{OBS}) and estimations of the drainage + runoff term (D + R) at Auradé and Lamasquère

	P (+I) [mm]	ΔSWC_{0_100} [mm]	ETR_{OBS} [mm]	[% of P (+I) - ΔSWC]	D + R [mm]	[% of P (+I) - ΔSWC]
Auradé						
winter wheat	397	-75	355	75	117	25
sunflower	374	-82	368	81	88	19
2005-2006	684	25	497	75	162	25
2006-2007	671	-100	564	73	207	27
Lamasquère						
maize	145 (+148)	-40	351	105	-18	-5
winter wheat	531	7	403	77	122	23
2005-2006	620 (+148)	43	609	84	116	16
2006-2007	615	-30	517	80	128	20

Table 6: Seasonal and annual cumulative values of observed ETR (ETR_{OBS}) and ETR simulated by the ICARE-SVAT model (ETR_{ICARE}), soil evaporation calculated with the marginal distribution sampling method (E_{MDS}) and by the ICARE-SVAT model (E_{ICARE}), and transpiration calculated with MDS (TR_{MDS}) and the ICARE-SVAT model (TR_{ICARE}) at Auradé and Lamasquère.

	ETR_{OBS} [mm]	ETR_{ICARE} [mm]	E_{MDS} [mm]	[% of ETR_{OBS}]	E_{ICARE} [mm]	TR_{MDS} [mm]	[% of ETR_{OBS}]	TR_{ICARE} [mm]
Auradé								
winter wheat	355	355	182	51	148	178	50	207
sunflower	368	403	208	57	224	163	44	179
2005-2006	497	518	324	65	307	178	36	212
2006-2007	564	608	404	72	429	163	29	179
Lamasquère								
maize	351	345	118	34	119	235	67	225
winter wheat	403	374	162	40	117	249	62	256
2005-2006	609	559	350	57	308	263	43	251
2006-2007	517	488	276	53	231	249	48	256